

Anharmonicity effects in polariton spectra of hyper-Raman scattering from calcite crystals

V. N. Denisov, B. N. Mavrin, V. B. Podobedov, and Kh. E. Sterin

Spectroscopy Institute, USSR Academy of Sciences

(Submitted 9 July 1981)

Zh. Eksp. Teor. Fiz. **82**, 406–420 (February 1982)

Fermi resonance of transverse and mixed E_u polaritons with bands of the two-phonon states $\nu_1 + \nu_2$ and $\nu_2 + \nu_3$ in a uniaxial centrosymmetric calcite crystal is investigated on the basis of the hyper-Raman scattering spectra. It is shown that, the conditions of formation of either a biphonon or quasibiphonon is always satisfied within the Agranovich-Lalov theoretical model for polariton Fermi resonance within the band of two-phonon states. Fermi-resonances between a polariton and biphonon or quasibiphonon are accompanied by the formation of a gap in the polariton spectrum, regardless of whether the biphonon becomes detached from the band or not. In Fermi resonance between a polariton and quasibiphonon the intensity of the polariton decreases and its width increases when the polariton frequency tends to frequency of the quasibiphonon. In the case of Fermi resonance between a polariton and group of two-phonon bands, the polariton intensity in the branches located between the bands should be appreciably lower than in the modes outside the band group. The resonances and anharmonic interaction constants of polaritons and two-phonon states are derived from the polariton spectra. The experimental data on polariton Fermi resonance (dispersion, intensity and line width of the polariton) are found to be in satisfactory agreement with the Agranovich-Lalov theory.

PACS numbers: 71.36. + c

I. INTRODUCTION

It is known that anharmonicity of oscillations can lead to a substantial restructuring of the vibrational spectrum of a crystal, particularly to the appearance, in second-order spectra, of bound (or quasibound) states of optical phonons (formation of biphonons or quasibiphonons).^{1,2} A particularly strong manifestation of anharmonicity takes place in polariton spectra. The polariton modes can cross the entire region of the elementary excitations of the crystal, including the region of the second-order spectrum. If the frequencies of the polaritons and of the second-order lines (two-phonon bands) are close, unharmonicity can produce a Fermi resonance between the polaritons and the two-phonon states (polariton Fermi resonance). Experimental^{3–11} and theoretical^{5,12,13} investigations have shown that the following effects can be observed in the case of polariton Fermi resonance: broadening of polariton lines, discontinuities in the polariton mode even in the absence of dipole biphonons in the second-order spectra, redistribution of the intensity in the scattering spectra, and deviations of the polariton dispersion from the calculated behavior that does not take into account the interaction of the polaritons with the two-phonon bands.

The behavior of the polaritons is particularly complicated inside two-particle state bands. According to Agranovich and Lalov (AL)¹³ a nonmonotonic polariton dispersion behavior is expected in the band, particularly "backtracking" of the dispersion curve that joins the individual polariton sections, as well as a discontinuity in the polariton curves in certain cases. The reverse sections of the polariton branch appear when account is taken of the critical points of the two-phonon state density, and have not yet been observed in experiment. It should be noted that the presence of damping makes it impossible for the two-phonon state density function to have either sharp boundaries or sharp breaks,¹⁴ and it seems that the role of the critical points is therefore

not always clearly pronounced in polariton spectra, especially in the dispersion curve.

The authors of experimental papers on polariton Fermi resonance have up to now interpreted the observed changes in the spectra only quantitatively. This is due both to the complexity of the phenomenon itself, which is burdened as a rule by superposition of two-phonon bands or by the proximity (at a distance of the order of the band width) of intense single-particle states in addition to polaritons, as well as by the scarcity of the experimental data, for example, on the density of two-particle states. A quantitative interpretation of polariton Fermi resonance might serve as a check on the validity of the theoretical models of polariton Fermi resonance. In addition, quantitative reduction of the experimental results would make it possible to determine the main parameters of the polariton Fermi resonance, namely the resonant-interaction constant Γ , which leads to a mixing of the polariton and two-phonon states, and the anharmonic-interaction constant A , which does not lead to a mixing of the polariton and two-phonon excitations, but is responsible for the interaction of the phonons with one another in the two-particle band.

Polariton Fermi resonance was investigated heretofore only by the Raman-scattering method, which made it possible to observe polaritons only in noncentrosymmetric crystals. We have shown¹⁵ that polaritons can be observed also in centrosymmetric crystals by the method of hyper-Raman scattering (HRS). In the HRS process the system is excited by two photons of frequency ω_i , and emits one photon $\omega_s = 2\omega_i \pm \omega$ (ω is the vibrational-excitation frequency). In analogy with Raman scattering (RS), one can introduce the crystal hyperpolarizability which determines, just as polarizability in the RS case, the intensity and the selection rules in HRS. The polarizability and hyperpolarizability are

tensors of second and third order, respectively. As a consequence, in HRS, in contrast to RS, the dipole oscillations, and hence the polaritons associated with them, are always active in both centrosymmetric and noncentrosymmetric crystals.

We investigate here, for the first time ever, the polariton Fermi resonance in the centrosymmetric calcite (CaCO_3) crystal by the HRS method. The vibrational spectra of the calcite crystal have been well investigated by various methods: RS,¹⁶ HRS,¹⁷ IR absorption,²⁴ and inelastic neutron scattering.¹⁸ The densities of the single-phonon and two-phonon states of calcite are known.¹⁹ Having such a diverse information, we have attempted to carry out a quantitative comparison of the experimental results with the predictions of the AL theory.¹³ In this connection, we present and analyze in part II of the paper the main results of the theory, which will be needed later to discuss the experimental data: dispersion, intensities and width of the polariton lines in the two-phonon state region. Attention is called to a fact that follows from the AL model,¹³ which was not discussed in that reference or elsewhere, and is of considerable importance for the interpretation of polariton Fermi resonances. The fact in question is that when the polariton branch crosses a two-phonon state band having the same symmetry as the polariton, a gap should always be produced in the polariton spectrum, regardless of whether a biphonon is detached or not. This gap is due to the interaction of the polariton either with a bound (non-decaying) state—biphonon—with a quasibound (decaying) state—a quasibiphonon. In part III of the paper we present our results of an experimental investigation of polariton HRS spectra of calcite in the region of the two-phonon bands $\nu_3 + \nu_3$ and $\nu_1 + \nu_3$. These results are compared with the predictions of the AL theory.¹³

II. FEATURES OF POLARITON FERMI RESONANCE WITHIN THE FRAMEWORK OF THE AL MODEL¹³

1. Polariton on dispersion. Fermi resonance of polariton with biphonon and with quasibiphonon

In the region of the two-phonon band, the polariton spectrum is completely defined by a Green's function $G(\omega, \mathbf{k})$ that takes into account resonant and anharmonic interaction of polaritons and two-phonon states¹³:

$$G(\omega, \mathbf{k}) = 2g(\omega) / [1 + \bar{A}(\omega, \mathbf{k})g(\omega)], \quad (1)$$

where $g(\omega)$ is the Green's function of the two free phonons that make up the two-particle band, without allowance for the resonant and anharmonic interaction,

$$\bar{A}(\omega, \mathbf{k}) = 2(A - \Gamma^2 u^2 / [\omega - \omega_p(\mathbf{k})]). \quad (2)$$

Here A is the anharmonic-interaction constant ($A > 0$ corresponds to phonon attraction and $A < 0$ to their repulsion), Γ is the constant of the resonant interaction of the polariton with the two-phonon states ($\Gamma > 0$), u^2 is the fraction of the mechanical energy in the polariton at the frequency ω ($0 < u^2 < 1$), and $\omega_p(\mathbf{k})$ is the frequency expected for a polariton with wave vector \mathbf{k} when no account is taken of the anharmonicity.

The dispersion of the polaritons is determined by the

position of the maximum of the polariton state density, i.e., by the maximum of the imaginary part of $G(\omega, \mathbf{k})$:

$$\text{Im } G(\omega, \mathbf{k}) = \frac{2 \text{Im } g(\omega)}{1 + 2\bar{A}(\omega, \mathbf{k}) \text{Re } g(\omega) + [\bar{A}(\omega, \mathbf{k})]^2 |g(\omega)|^2}. \quad (3)$$

The condition that $\text{Im } G(\omega, \mathbf{k})$ be a maximum determines the dispersion law $\omega(\mathbf{k})$ of the polaritons in the region of the two-phonon states¹³:

$$\omega(\mathbf{k}) = \omega_p(\mathbf{k}) + f(\omega), \quad (4)$$

$$f(\omega) = \Gamma^2 u^2 / [B(\omega) + A], \quad (5)$$

$$B(\omega) = \text{Re } g(\omega) / |g(\omega)|^2. \quad (6)$$

The imaginary and real parts of the Green's function $g(\omega)$ are uniquely connected with the spectrum of the two-phonon state density $\rho(\omega)$, normalized to unity area:

$$\text{Re } g(\omega) = \int \frac{\rho(\omega') d\omega'}{\omega - \omega'}, \quad \text{Im } g(\omega) = \pi \rho(\omega). \quad (7)$$

$\rho(\omega)$ should be taken to be the state density of a two-phonon band which is not perturbed by the anharmonic interaction of the oscillations.

We discuss now the distinguishing features of the polariton dispersion law (4). The function $f(\omega)$ in (4) determines the deviation of the dispersion $\omega(\mathbf{k})$, which takes into account the anharmonic interaction of the oscillations, from the dispersion $\omega_p(\mathbf{k})$ when no anharmonicity is taken into account. It becomes infinite at a frequency ω_f which is the solution of the equation

$$B(\omega_f) = 0. \quad (8)$$

In what follows, it is important that Eq. (8) coincides with the condition for the formation of a biphonon or a quasibiphonon, depending on the anharmonicity.^{1,2,14} If the frequency ω_f is outside the two particle band, then it coincides with the biphonon frequency. On the other hand, if ω_f lies in the region of the two-particle band, it coincides with the quasibiphonon frequency.

We note certain general features of the function $B(\omega)$, which do not depend on the specific form of the function $\rho(\omega)$. First, within the two-particle state band there exists at least one frequency ω_0 such that $B(\omega_0) = 0$ (Fig. 1). For simplicity we consider the most frequently encountered case of a single-hump density curve $\rho(\omega)$ [Fig. 1(b)]. In this case the position of the frequency ω_0 is close to the center of gravity of the density $\rho(\omega)$. It is seen from Fig. 1(a) that $B(\omega) < 0$ at $\omega < \omega_0$ and $B(\omega) > 0$ at $\omega > \omega_0$, and the modulus $|B(\omega)|$ increases with increasing detuning $|\omega - \omega_0|$. From the indicated properties of the function $B(\omega)$ it follows that the condition (8) can be satisfied independently of the magnitude and sign of the anharmonicity A . Consequently, if the anharmonicity is insufficient to detach a bound state—a biphonon—from the band, at least one quasibound state—quasibiphonon—is produced in the two-particle state band.

The properties of the function $B(\omega)$ determines the behavior of the function $f(\omega)$. Inasmuch as in the two-phonon band region the condition for the formation of a biphonon or of a quasibiphonon can be satisfied, there exists a frequency ω_f that coincides with the frequency

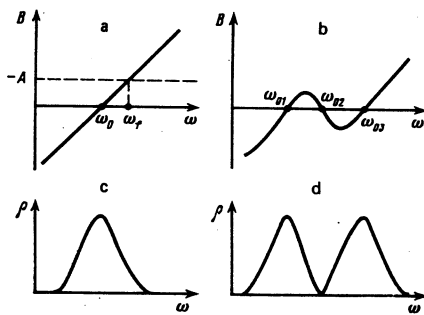


FIG. 1. Schematic form of the functions $B(\omega)$ (a, b) as functions of the shape of the contour of the two-particle state density $\rho(\omega)$ (c, d); ω_0 , ω_{01} , ω_{02} , and ω_{03} , are the frequencies at which $B(\omega) = 0$.

of the biphonon or quasibiphonon and satisfies the condition (8), under which $f(\omega)$ [the deviation of $\omega(\mathbf{k})$ from $\omega_p(\mathbf{k})$] becomes infinite. The sign of the function $f(\omega)$ is determined by the expression $B(\omega) + A$, which is negative at $\omega < \omega_f$ and positive at $\omega > \omega_f$. Therefore $f(\omega) \rightarrow -\infty$ as $\omega \rightarrow \omega_f$ from the left and $f(\omega) \rightarrow +\infty$ as $\omega \rightarrow \omega_f$ from the right. Far from the two-phonon band, as $|\omega - \omega_f| \rightarrow \infty$, the function $f(\omega) \rightarrow 0$, i.e., the $\omega(\mathbf{k})$ and $\omega_p(\mathbf{k})$ practically coincide.

Using the established properties of the function $f(\omega)$ it is easily seen from the polariton dispersion law (4) that a splitting of the polariton curve into two branches should always take place near the frequency ω_f (Fig. 2), namely the lower and upper branches 2 and 1, and a gap of width δ_k must be produced between them.

It follows thus from the AL model that the appearance of a gap in the polariton spectrum, in the region of the biphonon band, can be due to Fermi resonance between the polariton and either the biphonon or the quasibiphonon, and one of these possibilities can always be realized.

2. Intensity of polariton spectrum and polariton line width

At Fermi resonance, the intensity of the polariton spectrum in the region of two-phonon states is given by¹³

$$I(\omega) \sim \left[F + \frac{\Gamma u}{\omega - \omega_p(\mathbf{k})} D \right]^2 \text{Im} G(\omega, \mathbf{k}) = F^2 \left[\frac{\omega - \omega_a}{\omega - \omega_p(\mathbf{k})} \right]^2 \text{Im} G(\omega, \mathbf{k}), \quad (9)$$

where $\omega_a = \omega_p(\mathbf{k}) - \Gamma u D / F$, F and D are the matrix elements of the two-phonon and polariton transitions, re-

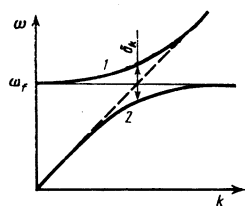


FIG. 2. Splitting of polariton curve into two branches at the Fermi resonance of the polariton with the biphonon (quasibiphonon). The symbols are explained in the text.

spectively. Thus, the intensity of the polariton spectrum is the result of interference of two-phonon states whose proper intensity is proportional to F^2 , with polariton states, whose intensity in the absence of polariton interaction with the two-particle band is proportional to D^2 .

Let us analyze the peak intensity (the intensity at the maximum) of the polariton lines in the two-particle state band. An expression for I_0 can be obtained by assuming in (9) that the frequency satisfies the dispersion law (4):

$$I_0(\omega) \sim F^2 |g(\omega)|^2 (\omega - \omega_a)^2 [B(\omega) + A]^2 / \Gamma^2 u^4 \text{Im} g(\omega). \quad (10)$$

It is seen that in the band $I_0(\omega) = 0$ at $\omega = \omega_a$ and $B(\omega) = -A$. Satisfaction of the condition $\omega = \omega_a$ is practically impossible, since it requires that the proper intensity of the two-particle states be of the order of the polariton intensity. The second condition $B(\omega) = -A$ can be realized if the anharmonicity is small and a quasibiphonon is produced. Consequently, at Fermi resonance between a polariton and a quasibiphonon, the peak intensity of the polariton tends to zero as $\omega \rightarrow \omega_f$, where ω_f is the frequency of the quasibiphonon.

Outside the two-particle-state band, expression (9) takes the form (we assume that $D \gg F$)

$$I(\omega) \sim D^2 \Gamma^2 u^2 \{ |A[\omega - \omega_p(\mathbf{k})] - \Gamma^2 u^2| |1 + 2A \text{Re} g(\omega) + 2[A(\omega - \omega_p(\mathbf{k})) - \Gamma^2 u^2] d \text{Re} g(\omega) / d\omega \}^{-1}, \quad (11)$$

where the frequency ω is a solution of Eq. (4). Attention must be called to the fact that outside the band the polariton intensity can still differ quite strongly from the intensity expected in the absence of an interaction of the polariton with the two-particle band.

In the two-particle-states band, a new channel is produced for the decay of a polariton into two phonons, as a result of which the polariton line should broaden. According to Refs. 2 and 14, the width $\Delta(\omega)$ of the polariton line in the band is

$$\Delta(\omega) = \Delta_p(\omega) + 2\Gamma^2 u^2 \text{Im} G_0(\omega), \quad (12)$$

where $\Delta_p(\omega)$ is the expected width of the polariton line in the absence of interaction of the polariton with the two-particle states, and $G_0(\omega)$ is the Green's function (1) at $\Gamma = 0$. We note that the frequency ω_f of the quasibiphonon is a pole of the function $G_0(\omega)$ (Refs. 13, 14). Consequently, as $\omega \rightarrow \omega_f$, the polariton line width increases strongly.

III. EXPERIMENTAL PART

1. Experimental procedure

Since the hyperpolarizability is small, the HRS is intense enough to be registered only in the case of strong excitation fields ($\sim 10^6$ V/cm), which are produced by pulsed lasers. The HRS spectra of calcite were excited by the 1064 nm line of a pulsed AYG laser and registered by a previously described²⁰ multichannel photoelectric spectrometer. Owing to the low dielectric-breakdown threshold of calcite, the peak intensity of the laser pulses did not exceed $2 \cdot 10^4$ W. The laser radiation was focused into the crystal by lenses of focal

length $F = 6$ cm at a scattering angle $\theta = 90^\circ$ and $F = 24$ cm at small angles θ . To decrease the level of scattered light in the spectrometer, the exciting radiation passing through the crystal was cut off with an interference light filter, which transmitted the HRS radiation. The HRS spectra were obtained at a spectral width of the gap ~ 10 cm $^{-1}$.

We have investigated, for the first time ever, HRS on polaritons in calcite. It is known^{3-11,15,21,22} that polaritons are observed at small scattering angles θ . To observe light scattered at small angles θ we used a scheme with annular diaphragms.¹⁵ The annular diaphragm was located at a distance ~ 100 mm from the crystal in such a way that the center of the annular slits coincided strictly with the axis of the exciting ray passing through the crystal. The average radius of the ring and the distance from the crystal to the diaphragm determined the scattering angle θ , and the width of the ring gap determined the angle $\Delta\theta$ in which the scattered light was gathered. In our experiment the angle $\Delta\theta$ was 0.2° , the laser-beam divergence did not exceed 0.3° inside the crystal. A set of diaphragms with different average ring radii was able to cover in discrete fashion the entire range of investigated scattering angles $\omega = 0-3^\circ$. We were thus able to measure the polariton functions $\omega(\theta)$. The energy and momentum conservation laws make it possible, knowing the dielectric constants of the crystal and the $\omega(\theta)$ dependence, to relate the angle θ with the magnitude of the wave vector k of the excited polaritons and consequently obtain the experimental polariton dispersion $\omega(k)$.¹⁵

Calcite is a centrosymmetric uniaxial crystal of the space group D_{3d}^6 with two formula units per unit cell. Active in its HRS spectra are the dipole vibrations $3A_{2u} + 5E_u$ and the $2A_{1u}$ vibrations which are forbidden in the IR and RS spectra.²³ In Table I are listed the line frequencies in the HRS spectra of calcite, measured by us at scattering angles $\theta = 90^\circ$. In Ref. 17 they observed in the HRS of calcite only three lines (90, 100, and 125 cm $^{-1}$) which were known earlier from the IR spectra. We have observed many more lines active in the IR spectrum. Moreover, we have succeeded in observing lines of the forbidden A_{1u} oscillations. Certain IR-active oscillation turned out to be very weak in our spectra, and their frequencies listed in Table I were taken from Ref. 24 (they are marked by asterisks).

TABLE I. Frequencies (in cm $^{-1}$) of the vibrational spectrum of a calcite crystal and their identification.

External oscillations		Internal oscillations	
92, 136	$A_{2u}(T), A_{2u}(L)$	712*, 715*	$E_u(T), E_u(L)$
101, 123	$E_u(T), E_u(L)$	714	E_g
156	E_g	873, 890*	$A_{2u}(T), A_{2u}(L)$
223, 239	$E_u(T), E_u(L)$	1085	A_{1u}
227	A_{1u}	1088	A_{1g}
283	E_g	1407, 1549	$E_u(T), E_u(L)$
297*, 384	$E_u(T), E_u(L)$	1432	E_g
300, 387*	$A_{2u}(T), A_{2u}(L)$		

Note. The frequencies of the A_{1g} and E_g oscillations were taken from Ref. 16; asterisks mark frequencies taken from Ref. 24.

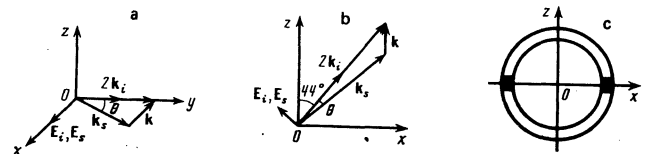


FIG. 3. Geometry of scattering by transverse (a) and mixed (b) polaritons in calcite; k_i and k_s are the wave vectors and E_i and E_s are the electric vectors of the exciting (i) and scattered (s) light; c) placement of the annular diaphragm relative to the crystallographic axes for the case a. Dark sections—locations of concentration of the light scattered by transverse polaritons.

The polaritons in the calcite were investigated by us in two scattering geometries (Fig. 3). In the first geometry— $y(xxx)y$ —the exciting radiation, polarized along the x axis, was directed along the y axis [Fig. 3(a)]. In this case the polaritons of noticeable intensity were concentrated only near the xy plane, so that annular diaphragms could be used [Fig. 3(c)]. According to the selection rules,²³ in such a scattering geometry only transverse E_u polaritons are active.

In the other geometry [Fig. 3(b)], the direction of the exciting radiation, polarized in the xz plane, was in the same xz plane and made an angle 44° with the z axis. The scattered radiation was concentrated also near the xz plane and in the interval of small scattering angles ($\theta < 2^\circ$). At the given geometry, the wave vector k of the polariton made an angle $\phi \neq 90^\circ$ with the z axis. In addition, the scattered radiation was polarized in the xz plane. Mixed polaritons were therefore excited in this case.

In the present study we investigated upper-branch polaritons in the frequency region 2000–3500 cm $^{-1}$. In this region of the vibrational spectrum of calcite there can be located only overtones and composite tones of the internal vibrations of the CO_3^{2-} group of calcite (see Table I). From among these, only the dipole-active two-phonon states of the same symmetry as the polariton can interact with the polaritons. We note that in

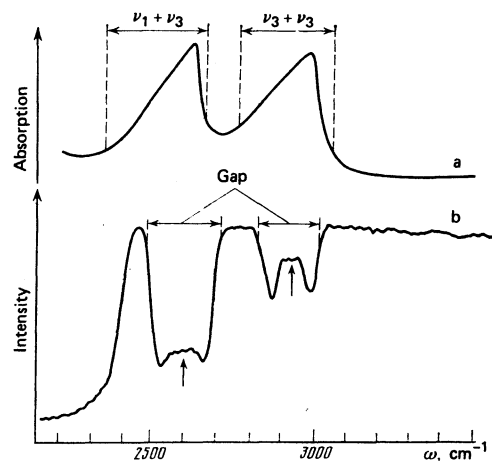


FIG. 4. IR absorption spectra at $E \perp z$ (a) and integrated HRS spectrum of transverse E_u polaritons ($\theta = 0-3^\circ$) (b) of a calcite crystal. The arrows indicate the broad maxima inside the gaps.

centosymmetric crystals, such as calcite, the overtones are not dipole-active.

In the region $\omega > 2400 \text{ cm}^{-1}$ of the IR absorption spectra of calcite, only two intense and asymmetrical bands of symmetry E_u are observed, with maxima at 2620 and 2990 cm^{-1} [Fig. 4(a) and Ref. 19]. Since the form of these bands has been distorted in Ref. 19, Figs. 4(a) shows the calcite IR absorption spectrum obtained by us as room temperature. Our analysis of the selection rules in the second-order spectra of calcite has shown that two groups of composite tones of symmetry E_u can be dipole-active in the region $\omega > 2400 \text{ cm}^{-1}$, namely

$$\nu_1 + \nu_3 \{A_{1u} \otimes E_u, A_{1u} \otimes E_u(T), A_{1u} \otimes E_u(L)\} \text{ and } \nu_3 + \nu_3 \{E_g \otimes E_u(T), E_g \otimes E_u(L)\}.$$

In accordance with Table I and Ref. 19, the 2620 and 2990 cm^{-1} bands of the IR spectrum [Fig. 4(a)] can be associated with these two groups of composite tones: $\nu_1 + \nu_3$ (three two-phonon bands) and $\nu_3 + \nu_3$ (two bands). It follows from spectroscopic investigations²⁴ and calculations¹⁹ that the $\nu_1(A_{1u})$ and $\nu_1(a_{1u})$ oscillations have a negligibly small dispersion in the entire Brillouin zone, while the oscillations $\nu_3(E_u(T))$, E_g , and $E_u(L)$ have a noticeable dispersion and form a "sandwich" of three practically non-overlapping bands with total width 145 cm^{-1} . The oscillation frequencies $\nu_1(A_{1u})$ and $\nu_1(a_{1u})$ almost coincide (see Table 1). Therefore the density of the two-phonons bands $\nu_1 + \nu_3$ coincides with the summary density of the one-phonon states ν_3 . The density of the two-phonon states $\nu_3 + \nu_3$ of symmetry E_u is governed by two bands: $E_g \otimes E_u(T)$ and $E_g \otimes E_u(L)$, while the state density of each band can be obtained by calculation. Thus, at $\omega > 2400 \text{ cm}^{-1}$ the polariton branch of the calcite crystal crosses two groups (two sandwiches) of two-phonon bands, each sandwich consisting of several (two or three) bands with known density of the two-particle states.

2. Fermi resonances in HRS spectra of transverse E_u polaritons

The Fermi-resonance gaps in the dispersion curves of the transverse E_u polaritons of calcites are easily observed even in the integrated HRS spectrum [Fig. 4(b)], i.e., in a spectral obtained with a large gathering angle $\Delta\theta$ of the scattered light ($\theta = 0-3^\circ$). Taking into account the exceeding low intensity of the spectra of HRS by polaritons, it is advisable to begin the search for possible polariton Fermi resonances with similar integrated spectra.

In the absence of Fermi resonance on the upper branch, the polariton states form a continuous set of values $\omega(\mathbf{k})$. According to the requirements of the energy and momentum conservation laws, the transverse E_u polaritons are allowed in the HRS spectra of calcite starting with $\sim 2430 \text{ cm}^{-1}$. Therefore in the absence of Fermi resonance we would observe in the integrated HRS spectrum a continuous spectrum starting with 2430 cm^{-1} . In the case of Fermi resonance, a gap can be produced in the polariton spectrum and is due to the appearance of two branches at Fermi resonance (see

Fig. 2); it depends both on the magnitude of the interaction of the polariton with the two-phonon band and on the geometry of the experiment.²¹

Two gaps, each $\sim 200 \text{ cm}^{-1}$ wide, were observed in the integrated spectrum of the transverse E_u polaritons of calcite [Fig. 4(b)]. Weak broad maxima are seen inside the gaps. Each of the observed gaps coincides with one of the sandwiches $\nu_1 + \nu_3$ or $\nu_3 + \nu_3$ (Fig. 4). We did not succeed in observing in the HRS spectra at $\theta = 90^\circ$ any lines whatever in the region of the sandwiches $\nu_1 + \nu_3$ and $\nu_3 + \nu_3$, although the scattered light was gathered from a much larger solid angle than in the geometry at small angles. This is evidence of a negligibly low proper intensity of the two-phonon transitions that participate in the polariton Fermi resonance.

In the polariton spectra obtained at different angles θ and with larger angular resolution $\Delta\theta$ ($\sim 0.2^\circ$) one can see near both gaps typical features of Fermi resonance (Fig. 5), namely the appearance of new resonances, a characteristic redistribution of the intensity among the branches, and the tendency of the frequencies of certain branches to a definite limit with changing angle θ .

Using the values of the refractive indices of calcite for the exciting (ω_i) and scattered ($\omega_s = 2\omega_i - \omega$) radiations²⁵

$$n(\omega_i) = 1.6423, \quad n(\omega_s) = 1.6628 - 0.0000025\omega,$$

the dielectric constant $\epsilon_\infty = 2.7$ (Ref. 24), the frequencies of the E_u oscillations (Table I), and the frequency-angle spectra $\omega(\theta)$ (Fig. 5), we obtained for the transverse E_u polaritons the experimental $\omega_e(k)$ dependences and calculated the theoretical dispersion curves $\omega_d(k)$ without allowance for the two-particle states (Fig. 6). It is seen from Fig. 6 that near the two-phonon bands $\nu_1 + \nu_3$ and $\nu_3 + \nu_3$ the experimental dependences $\omega_e(k)$ deviate strongly from the calculated $\omega_d(k)$ curves. We examine now the features of the discussed polariton Fermi resonances (Figs. 5 and 6).

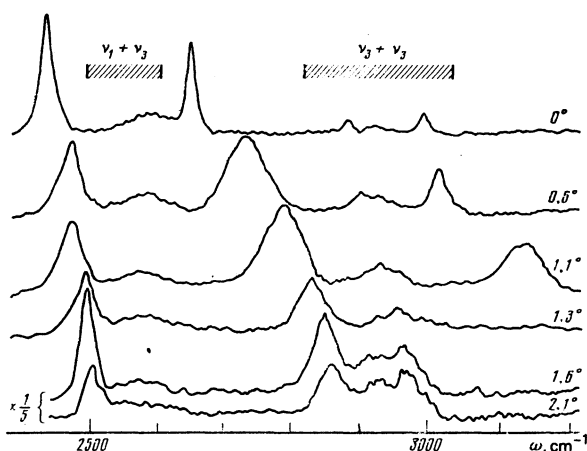


FIG. 5. HRS spectra of transverse E_u polaritons in a calcite crystal at various scattering angles θ . Scattering geometry $\nu(xxx)\nu$ (see Fig. 3a).

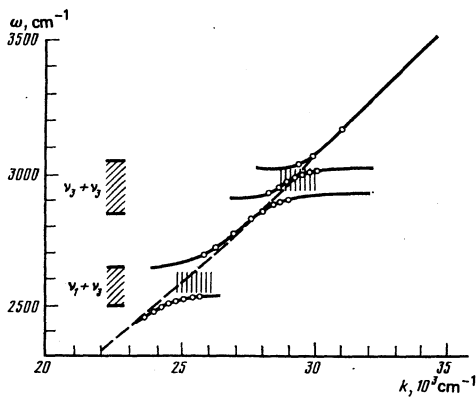


FIG. 6. Dispersion curves in calcite crystals; points—measured values of $\omega_p(k)$; dashed line—dispersion of polaritons $\omega_p(k)$ without allowance for two-particle states; solid lines—plots of $\omega(k)$ with allowance for the interaction of polaritons with two-phonon bands; the shaded regions correspond to broad unresolved regions inside the sandwiches.

As might be expected, in the region of the sandwich $\nu_3 + \nu_3$, which consists of two bands, namely $E_g \otimes E_u(T)$ (2830–2920 cm^{-1}) and $E_g \otimes E_u(L)$ (2870–3040 cm^{-1}) [Fig. 7(a)], polariton resonances with each band are observed. As a result, three branches are seen in the spectrum, lower (below 2870 cm^{-1}), middle (2900–2980 cm^{-1}), and upper (above 3005 cm^{-1}). In addition, a broad (2940 cm^{-1}) maximum is observed, which does not shift when the angle θ is changed and probably per-

tains to the two-phonon states, which can only be enhanced by the interaction with the polariton.

In the region of the sandwich $\nu_3 + \nu_3$, with increasing θ , the lower branch of the first resonance tends to a definite frequency, which lies inside the first band [$E_g \otimes E_u(T)$] of the sandwich. The frequency of the resonance with the second band lies inside the second two-particle band $E_g \otimes E_u(L)$. Therefore, within the framework of the AL model, the observed resonances in the region of the sandwich $\nu_3 + \nu_3$ should be due to the interaction of the polariton with quasibiphonons of the first and second bands. We note that the lower branch of the Fermi resonance with the sandwich $\nu_1 + \nu_3$ also tends to a frequency that lies inside the lower band of the two-particle states of this sandwich.

Another feature of polariton resonances with the sandwiches $\nu_1 + \nu_3$ and $\nu_3 + \nu_3$ is that the intensity of the polariton branches, which lie between the bands (middle branches) is much less than the intensity of the lower and upper branches. Therefore when the polariton is at resonance with the sandwich $\nu_1 + \nu_3$ we are able to observe with assurance only the lower and upper branches. In the region of the resonance of the polariton with the sandwich $\nu_3 + \nu_3$, the scattering in the region of the middle branch, while observed, was weaker than for other branches.

We shall use below the density of the two-phonon states, which is known from the literature, and the $\omega_p(k)$ dependence to determine the interaction constants Γ and A of ordinary polaritons with quasibiphonons of the $\nu_3 + \nu_3$ band. Next, using the obtained constants, we calculate the course of the polariton branches $\omega(k)$ in the region of the sandwich $\nu_3 + \nu_3$, and also the widths and intensities of the polariton lines in the bands of the two-particle states $\nu_3 + \nu_3$ and compare the results of the calculations with the measurement data. By the same token, we check on the correctness of description of the polariton Fermi resonance with the aid of the AL model.

3. Determination of the anharmonicity constants and comparison of the experimental results with those predicted by the AL model

To determine the constants of the interaction of the polaritons with the two-particle bands $\nu_3 + \nu_3$ it suffices to know the positions ω_1 and ω_2 of the maximum of the polariton at any two angles θ_1 and θ_2 of the scattering by polariton branches of each resonance. It follows then from the dispersion law (4) that

$$A = \frac{K_2 B(\omega_2) - K_1 B(\omega_1)}{K_1 - K_2}, \quad \Gamma^2 = K_1 [B(\omega_1) + A] = K_2 [B(\omega_2) + A], \quad (13)$$

where

$$K_1 = [\omega_1 - \omega_p(\theta_1)]/u^2, \quad K_2 = [\omega_2 - \omega_p(\theta_2)]/u^2.$$

The phonon fraction u^2 in the polariton is obtained in the usual manner.²⁶ The function $B(\omega)$ [Fig. 7(b)] is determined by the density $\rho(\omega)$ of the two-particle states [Fig. 7(a)] with the aid of Eqs. (6) and (7).

The polariton dispersion in the region of the sandwich $\nu_3 + \nu_3$ is determined by the interaction of the po-

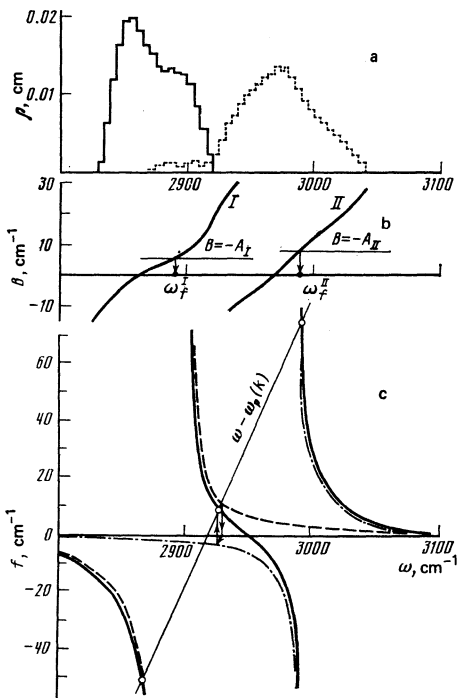


FIG. 7. Density functions of two-phonon states $\rho(\omega)$ of the first (solid line) and second (dashed) band in the sandwich $\nu_3 + \nu_3$ of a calcite crystal (a); calculation of the function $B(\omega)$: I) for the first band and II) for the second band (b); (c) dashed line—the function $f_I(\omega)$, dashed-dot— $f_{II}(\omega)$ and solid line— $f(\omega)$. The arrows show the method of constructing the symmetry function $f(\omega)$.

laritons with two bands, while below the sandwich the main contribution is made by the first band $E_f \otimes E_u(T)$, and above the sandwich by the band $E_f \otimes E_u(L)$. Inside the sandwich, both bands can make equal contributions. Therefore, when determining the anharmonicity constants for the first band we used the experimental points of the lower branch, while for the second band we use the points of the upper branch. The calculated constants of the interaction of the polaritons with the bands $E_f \otimes E_u(T)$ and $E_f \otimes E_u(L)$ are given in Table II. According to the classification of Ref. 14, the resonant and anharmonic interactions of the polaritons with a band $\nu_3 + \nu_3$ turn out to be weak, since $\Gamma u/T$ and $|A|/T < 0.2$ (T is the width of the band). In this case, no biphonons can be produced. This agrees with the conclusions of Sec. III.2 that the observed singularities in the region of the sandwich $\nu_3 + \nu_3$ are connected with the interaction of the polariton with the quasibiphonons of the bands. The obtained negative values of the constants A (Table II) are evidence of the mutual repulsion of the phonons that make up the two-particle bands.

Knowing the constants A and Γ , we can obtain the dispersion relation $\omega(k)$ that takes into account the interaction of the polaritons with the two-particle states. The $\omega(k)$ dependence is determined graphically in the following manner. We plot first the functions

$$f_I(\omega) = \Gamma_I^2 u_I^2 / [B_I(\omega) + A_I], \quad f_{II}(\omega) = \Gamma_{II}^2 u_{II}^2 / [B_{II}(\omega) + A_{II}],$$

where the subscripts I and II pertain respectively to the first and second bands of the sandwich $\nu_3 + \nu_3$. According to (4), the functions $f_I(\omega)$ and $f_{II}(\omega)$ specify the partial contributions of each band to the total deviation $f(\omega)$ of the dispersion curve $\omega(k)$ from $\omega_A(k)$ [$f(\omega) = \omega - \omega_A(k)$]. When the total deviation $f(\omega)$ is determined, successive account is taken of the interaction first with the first band and then with the second. The function $f(\omega)$ can be easily constructed graphically [Fig. 7(c)].

The points of intersection of the plot of $f(\omega)$ and the straight lines $\omega - \omega_A(k)$ determine the unknown frequencies $\omega(k)$. The $\omega(k)$ dependence is shown in Fig. 6 by the solid line. It is seen that the anharmonicity constants determined by us can describe satisfactorily the experimental dispersion curves obtained when polaritons are at resonance with the band $\nu_3 + \nu_3$.

We discuss now other features of the Fermi resonances in the region of the sandwich $\nu_3 + \nu_3$.

1) It was noted above that at Fermi resonances of the polaritons with the sandwich $\nu_3 + \nu_3$ the intensity of the polaritons on the middle branch turned out to be lower than on the lower and on the upper branches (Fig. 5). This decrease can be explained within the framework of the AL model. Indeed, the intensity that the polariton

would have in the absence of its interaction with the two-particle bands decreases considerably as a result of the Fermi resonance, and even tends to zero as $\omega - \omega_f$ [Eqs. (10) and (11)]. In our case, the decrease of the polariton intensity is due to the combined contribution of the two bands of the sandwich $\nu_3 + \nu_3$. It is easily seen that the polariton intensity is small on the lower part of the middle branch, since the frequency of the polariton is close to the quasibiphonon frequency ω_f^I , while on its upper branch it is close to ω_f^{II} . Therefore, the expected intensity of the polaritons of the middle branch is always lower than on the lower and upper branches where the influence of only one nearest band manifests itself in the main. These qualitative considerations are confirmed by quantitative estimates that agree with experiment. Thus, when the polariton branch crosses a group of bands (a sandwich) the intensity of the polaritons on the middle branches should always decrease.

2) The measurement of the polariton-line widths is made complicated as is well known, by the fact that instrumental function contains a component that depends on the angle $\Delta\theta$ into which the scattered light is gathered.²² It is not always possible to take a correct account of this component. We were therefore able to measure the polariton line width only in those sections of the polariton branches where the contribution of $\Delta\theta$ could be neglected. Table III lists the polariton line widths Δ at the frequency 2865 cm^{-1} as determined by experiment and calculated by Eq. (12). It is seen that the line width is satisfactorily described within the framework of the AL model. We note that if no account were taken of the two-particle states, the width $\Delta_A(\omega)$ would be approximately 1 cm^{-1} and only because of the interaction with these states is the line broadened to 41 cm^{-1} .

3) The finite gathering angle $\Delta\theta$ makes it also difficult to determine correction the polariton intensity. Figure 8 shows the frequency dependence of the peak intensity $I_0(\omega)$ of the polaritons on that section of $\omega_s(k)$ where the intensities are least subject to distortion on account of the finite angle $\Delta\theta$. It is seen that the measurement results (points) correlate satisfactorily with the calculated $I_0(\omega)$ dependences (solid line) calculated from Eq. (10). The scale for the calculated curve was chosen such that the curve passes through the experimental point at $\omega = 2865 \text{ cm}^{-1}$.

4) It is seen from Figs. 4 and 7(a) that the contours of the IR absorption band $\nu_3 + \nu_3$ and of the density $\rho(\omega)$ of the dipole-active states of this sandwich are different. Generally speaking, this disparity can be due to

TABLE II. Parameters of Eqs. (13) for the calculation of the bandwidths T and of the constant of interactions of the polaritons with the two-particle bands $\nu_3 + \nu_3$ of a calcite crystal.

$\nu_3 + \nu_3$	u^2	T, cm^{-1}	ω_1, cm^{-1}	ω_2, cm^{-1}	K_1, cm^{-1}	K_2, cm^{-1}	Γ, cm^{-1}	A, cm^{-1}
$E_f \otimes E_u(T)$	0.11	90	2830	2865	-136	-364	40.5	-5.5
$E_f \otimes E_u(L)$	0.11	120	3005	3035	272	92	36	-7.5

TABLE III. Widths of polariton lines [calculated from Eq. (12) and obtained from experiment] and the imaginary part of the Green's function $G_0(\omega)$ in the bands of the two-particle states of a calcite crystal.

Composite tone	ω, cm^{-1}	$\text{Im } G_0(\omega), 10^{-2} \text{ cm}^{-1}$	Δ, cm^{-1}	
			Calculation	Experiment
$E_f \otimes E_u(T)$	2865	4.9	38	41
$A_{1g} \otimes E_u(T)$	2500	7.3	33	34

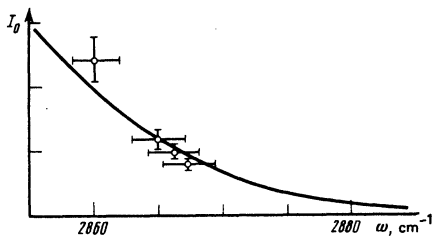


FIG. 8. Peak intensity I_0 of polariton vs. frequency in the two-particle state band $E_f \otimes E_u(T)$ of the sandwich $\nu_3 + \nu_3$ in a calcite crystal.

the unharmonic interaction of the phonons.^{14,27} In the case when a quasibiphonon is produced, the maximum of the absorption band can coincide with the position of the quasibiphonon. The quasibiphonon frequencies are solutions of Eq. (8), and it follows from Fig. 7(b) that they amount of $\omega_f^I = 2894 \text{ cm}^{-1}$ in the first band and $\omega_f^{II} = 2990 \text{ cm}^{-1}$ in the second. The quasibiphonon frequency 2990 cm^{-1} ($E_f \otimes E_u(L)$) coincides with the position of the maximum of the IR absorption band. The absence of other maxima from the $\nu_3 + \nu_3$ band may indicate that the two-particle states of the first band manifest themselves weakly in the IR spectrum and are revealed only by the fact that the 2990 cm^{-1} absorption band is asymmetric. Thus, the considered features of the polariton Fermi resonance not only do not contradict the IR-absorption data, but offer also a possible explanation of the absorption line shape.

Although the quantitative features of the polariton Fermi resonance with the sandwich $\nu_1 + \nu_3$ are the same as with $\nu_3 + \nu_3$ a complete quantitative interpretation is made difficult by the fact that the sandwich $\nu_1 + \nu_3$ contains three bands and there should be two middle branches, whose dispersion we did not succeed in measuring. Reduction of the experimental polariton curves in the region of the sandwich $\nu_1 + \nu_3$ has made it possible only to establish the position of the quasibiphonons in the first and third bands, 2508 and 2620 cm^{-1} . The position of the 2620 cm^{-1} quasibiphonon [$A_{1g} \otimes E_u(L)$] copolaritons in a scattering geometry of Fig. 3(b) turn

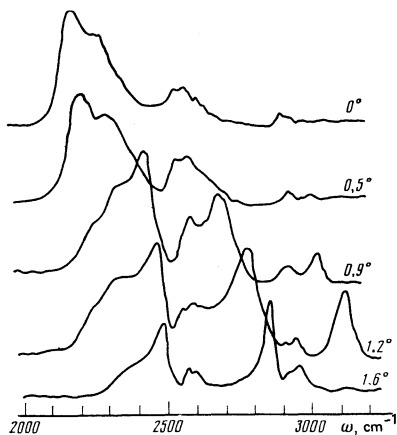


FIG. 9. HRS spectra of mixed E_u polaritons in a calcite crystal at different scattering angles θ . The scattering geometry is indicated in Fig. 3b.

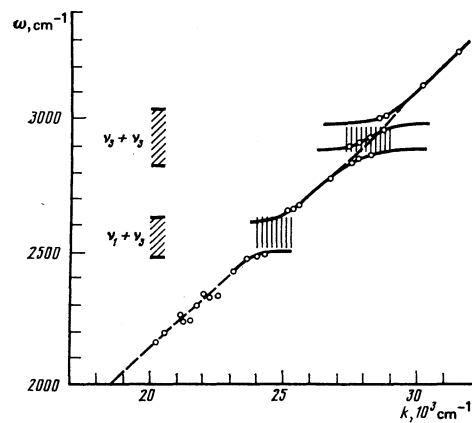


FIG. 10. Dispersion curves of mixed polaritons in a calcite crystal. The notation is the same as in Fig. 6.

out to be allowed starting with 2160 cm^{-1} (Fig. 9). This has made it possible to reserve two more polariton incidences with the IR absorption maximum (see Fig. 4). It is probable that a composite tone of the phonons, one of which is longitudinal [$E_u(L)$], manifests itself most strongly in the IR spectra of the sandwich $\nu_1 + \nu_3$, just as in $\nu_3 + \nu_3$. A comparison of the measured polariton line widths at the frequency 2500 cm^{-1} , measured and calculated by formula (12) in the region of the sandwich $\nu_1 + \nu_3$ has shown that they agree satisfactorily with each other, just as in the case of the $\nu_3 + \nu_3$ sandwich (Table III).

4. Fermi resonances in HRS spectra of mixed polaritons

It is known²⁸ that mixed polaritons contain a smaller fraction of E_u oscillations than the transverse E_u polaritons. Therefore the resonance interaction between a mixed polariton and two-particle states is expected to be smaller.

Whereas the transverse polaritons of calcites are resolved in the HRS starting with 2430 cm^{-1} , mixed Fermi resonances, near 2260 and 2360 cm^{-1} , which were poorly resolved in our experiments and turned out to be close to the maxima of the weak two-phonon IR absorption bands with symmetry E_u , namely 2240 and 2335 cm^{-1} (Ref. 19).

It is from the dispersion curves of the mixed polaritons (Fig. 10) that the experimental points deviate very slightly from the $\omega(k)$ curve calculated for the mixed polaritons by an iteration method²⁹ without allowance for the interaction with the two-phonon states. Estimates have shown that at the anharmonicity values A taken from Table II the experimental points agree best with the calculated $\omega(k)$ curves if the resonant-interaction constants are taken to be the values of $\Gamma \sin \phi$, where Γ is taken from Table II and ϕ is the angle between the polariton wave vector and the z axis. In the region 2400 cm^{-1} the angle ϕ varied insignificantly and was close to 30° .

The author thanks V.M. Agranovich for interest in the present work and for a number of valuable discussions.

- ¹V. M. Agranovich, Fiz. Tverd. Tela (Leningrad) **12**, 562 (1970) [Sov. Phys. Solid State **12**, 430 (1970)].
- ²J. Ruvalds and A. Zawadowski, Phys. Rev. **B2**, 1172 (1970).
- ³B. N. Mavrin and Kh. E. Sterin, Pis'ma Zh. Eksp. Teor. Fiz. **16**, 265 (1972) [JETP Lett. **16**, 187 (1972)]. Fiz. Tverd. Tela (Leningrad) **18**, 3028 (1976) [Sov. Phys. Solid State **18**, 1764 (1976)].
- ⁴F. K. Winter and R. Claus, Opt. comm. **6**, 22 (1972); **22**, 318 (1977).
- ⁵D. N. Klyshko, V. F. Kutsov, A. N. Penin, and B. F. Polkovnikov, Zh. Eksp. Teor. Fiz. **62**, 1846 (1972) [Sov. Phys. JETP **35**, 960 (1972)].
- ⁶K. D. Kneipp, G. É. Ponat, V. L. Strizhevskii, and Yu. N. Yashkir, Pis'ma Zh. Eksp. Teor. Fiz. **18**, 89 (1973) [JETP Lett. **18**, 50 (1973)].
- ⁷G. M. Georgiev, A. G. Mikhaïlovskii, A. N. Penin, and V. N. Chumash, Fiz. Tverd. Tela (Leningrad) **16**, 2907 (1974) [Sov. Phys. Solid State **16**, 1882 (1975)].
- ⁸G. G. Mitin, V. S. Gorelik, L. A. Kulevskii, Yu. N. Polivanov, and M. M. Sushchinskii, Zh. Eksp. Teor. Fiz. **68**, 1757 (1975) [Sov. Phys. JETP **41**, 882 (1975)]; V. S. Gorelik, G. G. Mitin, and Yu. N. Polivanov, *ibid.* **69**, 823 (1975) [**42**, 419 (1975)].
- ⁹O. A. Aktsipetrov, G. M. Georgiev, I. V. Matyusheva, A. G. Mikhaïlovskii, and A. N. Penin, Fiz. Tverd. Tela (Leningrad) **17**, 2027 (1975) **18**, 665 (1976) [Sov. Phys. Solid State **17**, 1342 (1975), **18**, 384 (1976)].
- ¹⁰Yu. N. Polivanov, Pis'ma Zh. Eksp. Teor. Fiz. **30**, 415 (1979) [JETP Lett. **30**, 388 (1979)].
- ¹¹V. N. Denisov, B. N. Mavrin, V. B. Podobedov, and Kh. E. Sterin, Opt. Comm. **34**, 337 (1980).
- ¹²V. L. Strizhevskii, G. É. Ponat, and Yu. N. Yashkir, Opt. Spektrosk. **31**, 388 (1971); **44**, 601 (1978).
- ¹³V. M. Agranovich and I. I. Lalov, Fiz. Tverd. Tela (Leningrad) **13**, 1032 (1971) [Sov. Phys. Solid State **13**, 859 (1971)] Zh. Eksp. Teor. Fiz. **61**, 656 (1971) [Sov. Phys. JETP **34**, 350 (1972)]; Sol. St. Comm. **19**, 503 (1976); V. M. Agranovich, E. P. Ivanova, and I. I. Lalov, Fiz. Tverd. Tela (Leningrad) **21**, 1629 (1979) [Sov. Phys. Solid State **21**, 935 (1979)].
- ¹⁴M. V. Belousov, D. E. Pogarev and S. V. Pogarev, in: Kolebaniya okisnykh reshetok (Oscillations of Oxide Lattices), A. N. Lazarev and M. O. Bulanin, eds., Nauka, 1980, p. 249.
- ¹⁵V. N. Denisov, B. N. Mavrin, V. B. Podobedov, and Kh. E. Sterin, Pis'ma Zh. Eksp. Teor. Fiz. **31**, 111 (1980) [JETP Lett. **31**, 101 (1980)].
- ¹⁶S. P. S. Porto, J. A. Giordmaine, and T. C. Damen, Phys. Rev. **147**, 608 (1966).
- ¹⁷Yu. N. Polivanov, and R. Sh. Sayakhov, Fiz. Tverd. Tela (Leningrad) **20**, 2708 (1978) [Sov. Phys. Solid State **20**, 1564 (1978)] Phys. Stat. Sol. (b) **103**, 89 (1981).
- ¹⁸E. R. Cowley and A. K. Pant, Phys. Rev. **B8**, 4795 (1973).
- ¹⁹M. Plihal, Phys. Stat. Sol. (b) **56**, 495 (1973).
- ²⁰V. N. Denisov, B. N. Mavrin, V. B. Podobedov, and Kh. E. Sterin, Zh. Eksp. Teor. Fiz. **75**, 684 (1978) [Sov. Phys. JETP **48**, 344 (1978)].
- ²¹Yu. N. Polivanov and K. A. Prokhorov, Fiz. Tverd. Tela (Leningrad) **21**, 3593 (1979) [Sov. Phys. Solid State **21**, 2074 (1979)].
- ²²B. N. Marvin and Kh. E. Sterin, *ibid.* **18**, 3653 (1976) [**18**, 2127 (1976)]. Zh. Prikl. Spekt. **27**, 896 (1977).
- ²³S. J. Cyvin, J. E. Rauch, and J. C. Decius, J. Chem. Phys. **43**, 4083 (1965).
- ²⁴K. H. Hellwege, W. Lesch, M. Plihal, and G. Shaak, Z. d. Physik **232**, 61 (1970).
- ²⁵E. M. Voronkova, B. N. Grechushnikov, G. I. Distler, and I. P. Petrov, Opticheskie materialy dlya infrakrasnoy tekhniki (Optical Materials for Infrared Technology), Nauka, 1965.
- ²⁶V. M. Agranovich and V. L. Ginzburg, Kristallogoptika s uchestom prostranstvennoi dispersii i teoriya éksitonov (Spatial Dispersion in Crystal Optics and the Theory of Excitons), Nauka, 1979, p. 516 [Wiley, 1967].
- ²⁷F. Bogani, J. Phys. C: **11**, 1297 (1978).
- ²⁸R. Loudon, Adv. Phys. **13**, 423 (1964).
- ²⁹F. X. Winter, E. Wiesendanger, and R. Claus, Phys. Stat. Sol. (b), **72**, 189 (1975).

Translated by J. G. Adashko